Type of article: Original Article

Evaluate the efficiency of Mr BMT in macrophage replacement of peripheral organs

Jinjin Du [1,3,#], Baozhi Yang [1,2,#], Yang He [3*], Yanxia Rao [2*]

Author affiliations:

[1] School of Basic Medical Sciences, Jinzhou Medical University, Jinzhou, Liaoning 121001, China

[2] Department of Neurology, Zhongshan Hospital, Department of Laboratory Animal Science, MOE Frontiers Center for Brain Science, Fudan University, Shanghai 200032, China

[3] Institute for Translational Brain Research, State Key Laboratory of Medical Neurobiology, MOE Frontier Center for Brain Science, Fudan University, Shanghai

[#] These authors contribute equally.

* Correspondence: 21111520009@m.fudan.edu.cn (Y.H.), yanxiarao@connect.hku.hk (Y.R.)

Total number of pages: 34

Total number of photographs: 8

Word counts: for abstract: 187, for the text: 6019

Competing Interests

The authors declare no competing financial interests.

Evaluate the efficiency of Mr BMT in macrophage replacement of peripheral organs

Abstract

The successful replacement of endogenous tissue-resident macrophages with healthy bone marrow-derived cells through transplantation presents a promising therapeutic approach for treating disease associated with macrophage dysfunction. Our previous development of the novel microglia replacement by bone marrow transplantation (Mr BMT) method achieved high engraftment efficiency in the central nervous system (CNS), overcoming the limitation of traditional bone marrow transplantation (tBMT). In this study, we aimed to investigate the potential impacts of Mr BMT approach on peripheral organs. The Mr BMT approach involves depleting resident microglia through colony stimulating factor-1 receptor (CSF-1R) inhibition, so we first evaluated the survival of peripheral macrophages after CSF-1R inhibition. We observed that the CSF-1R antagonist, PLX5622, exerted significant elimination of peripheral tissue macrophages, albeit with lower efficiency than in the CNS. Furthermore, we discovered that Mr BMT achieved replacement efficiencies comparable to tBMT in peripheral tissues such as the liver, kidney, lung, and spleen. Our findings suggested Mr BMT is a highly efficient strategy for allogeneic macrophage replacement in both the CNS and peripheral organs, and it could have potential clinical applications.

Key-words: microglia, macrophage, microglia replacement, Mr BMT, tBMT, CSF-1R

45 ***Introduction***

46 Tissue-resident macrophages, including microglia which are brain parenchyma resident macrophages,
47 continuously monitor and clear pathogens throughout the lifespan. The new paradigm suggests that
48 several tissue-resident macrophage populations are seeded during waves of embryonic
49 haematopoiesis and self-maintain independently of BM contribution during adulthood[1-3].
50 Microglia and other tissue-resident macrophages play essential roles in the development,
51 homeostasis, tissue repair, and disease defence both in the CNS and peripheral organs. Dysfunction
52 or genetic mutations have been linked to a wide range of diseases, including neurodegeneration,
53 autoimmune disorders, inflammation, and bone disease[4]. Allogeneic bone marrow and stem cell
54 transplantation are effective options for the treatment of inherited diseases of the immune system,
55 such as severe combined immunodeficiency (SCID)[5] and some autoimmune diseases, including
56 systemic lupus erythematosus (SLE)[6] , rheumatoid arthritis (RA)[7] , type 1 diabetes (T1D)[8] and
57 multiple sclerosis (MS)[9] . This approach involves replacing the recipient's bone marrow and
58 immune cells with healthy donor cells that can repopulate the immune system, leading to improved
59 disease outcomes.

60

61 We previously developed a novel strategy for nonself microglia replacement by bone marrow
62 transplantation at CNS-wide scale and named this procedure Mr BMT[10] . This involves first
63 depleting the resident microglia through either genetic or pharmacological means, followed by
64 transplantation of bone marrow cells that giving rise to new microglia. The existing microglia of
65 recipient mice will be replaced by microglia-like cell derived from bone marrow cells[11, 12] . This
66 strategy can be useful in cases where the resident microglia are dysfunctional and contribute to the
67 development of neurodegenerative, such as Alzheimer's disease (AD)[13] , Parkinson disease
68 (PD)[14] and Frontotemporal dementia (FTD)[15] . However, it is important to evaluate the potential
69 effects of Mr BMT on peripheral tissue macrophages when considering this therapy for clinical

translation, since the approach used for microglia ablation also have significant effects on the tissue macrophages and monocyte populations[16-18].

The current study observed highly effective tissue macrophage replacement in the liver, kidney, lung, and spleen after Mr BMT, indicating the potential of this therapy to have broad impacts on tissue macrophage populations throughout the peripheral organs. These encouraging results suggested that Mr BMT may be a promising cell therapy strategy for a wide range of diseases that affect both the central and peripheral immune systems, such as amyotrophic lateral sclerosis (ALS) and adrenoleukodystrophy (ALD).

Materials and Methods

Animals and PLX5622 administration

Cx3cr1-GFP (B6.129P2(Cg)-*Cx3cr1*^{tm1Litt}/J, Strain #: 005582) mice were purchased from the Jackson Laboratory (Shanghai, China)[19]. C57BL/6J mice were purchased from Charles River (Shanghai, China). All mice were housed in the Animal Facility at the Department of Laboratory Animal Science at Fudan University under a 12 hours light/dark cycle with food and water given ad libitum. All animal experiments were conducted in accordance with the guidelines of the Institutional Animal Care and Use Committee of the Department of Laboratory Animal Science at Fudan University (202009001S and 2021JS-NZHY-002). All PLX5622 were formulated in AIN-76A chow at a concentration of 1200 mg/kg (Cat# D20010801, SYSE Bio, Changzhou, China). PLX5622 group mice were fed with PLX5622 chow for 14 days ad libitum. Control diet group mice were fed with AIN-76A chow ad libitum.

Tissue preparation for the cryosection and immunohistochemistry

94 Mice were deeply anesthetized with isoflurane and were then subjected to transcranial perfusion with
95 50 ml of 0.01 M cold PBS or 0.9% NaCl. Next, all mice were perfused with 4% cold
96 paraformaldehyde (PFA) for fixation. The brains and peripheral organs, including liver, lung, kidney
97 and spleen were collected and postfixed in 4% PFA overnight (ON) at 4 °C or 6 hours in room
98 temperature (RT). All tissues were dehydrated by 30% sucrose in 0.01 M PBS in 4 °C for 2-3 days
99 and then embedded in optimal cutting temperature compound (OCT). All samples were stored at -
100 80 °C before cryosection. All tissues were frozen in the freezing microtome for 15 minutes before
101 cryosection. Tissues with regions of interest were sectioned by Leica CM1950 cryostat at 35 μm
102 thickness.
103
104 **Immunohistochemistry and image acquisition**
105 The sections of brain and peripheral organs were rinsed by 0.01 M PBS for 3 times. Next, brain and
106 peripheral organ sections were blocked and permeabilized with 0.01 M PBS containing 0.03% Triton
107 X-100 and 4% normal donkey serum (NDS) for 2 hours at RT. Next, the samples were incubated in
108 primary antibody in 1% NDS in PBST at 4 °C ON. After rinsed by 0.03% PBST for 3 times, the
109 samples were incubated fluorescent dyes conjugated secondary antibody in 1% NDS in PBST for 2
110 hours at RT, together with 1:500 4', 6-diamidino-2-phenylindole (DAPI). Next, samples were rinsed
111 by 0.03% PBST for 3 times and then mounted anti-fade mounting medium. The edge of the cover
112 glass was sealed with nail enamel.
113 Primary antibody information and concentration: rabbit anti-IBA1 (1:500, Cat# 019-19741, Wako,
114 Japan); goat anti-IBA1 (1:500, Cat# ab5076, Abcam, Cambridge, UK); goat anti-GFP (1:1000, Cat#
115 ab6673, Abcam, Cambridge, UK); rabbit anti-GFP (1:1000, Cat# A11122, Thermo Fisher,
116 Massachusetts, USA); rat anti-F4/80 (1:500, Biolegend, Cat# 123101, California, USA); mouse anti-
117 CD11c (1:500, Cat# 117314, Biolegend, California, USA). Secondary antibody information: Donkey
118 anti-rat 647 (1:1000, Cat# A48272, Invitrogen, California, USA); Donkey anti-rat 568 (1:1000, Cat#

119 ab175475, Abcam, Cambridge, UK); Donkey anti-rabbit 488 (1:1000, Cat# A11008, Thermo Fisher,
120 Massachusetts, USA); Donkey anti-goat 488 (1:1000, Cat# A11055, Thermo Fisher, Massachusetts,
121 USA); Donkey anti-rabbit 568 (1:1000, Cat# A10042, Thermo Fisher, Massachusetts, USA);
122 Donkey anti-rabbit 647 (1:1000, Cat# 711-605-152, Jackson, Pennsylvania, USA).
123 Confocal images were acquired by using an Olympus FV3000 confocal microscope with a solid-
124 state laser. Lasers with wavelengths of 405 nm, 488 nm, 561 nm, and 640 nm were used to excite the
125 fluorophores. Then, ×60 (oil), ×40 (oil), and ×20 objectives were utilized. Some whole-brain
126 fluorescence images were acquired by an Olympus VS120 microscope equipped with a motorized
127 stage. Then, ×10 objective was used. Z-stacked focal planes were acquired and maximally projected
128 with Fiji. The brightness and contrast of the image were adjusted with Fiji if necessary.
129
130 **Bone marrow cells preparation**
131 Bone marrow cells were collected from adult *Cx3cr1*$^{+/GFP}$ mice. In brief, femora and tibia were
132 collected and the muscles were removed. Next, the bones were placed in cold 0.01 M PBS and
133 washed twice. After that, bone marrow cells were collected using 10 mL syringe with a 26-gague
134 needle. Next, cells were washed by L15 medium containing 10% FBS and centrifuged at 300 g for
135 10 minutes. Cell pellets were then resuspended with L15 medium containing 10% FBS and passed
136 through 40 μm cell strainers. After that, cell number was counted, and bone marrow cells were
137 diluted in appropriate amount medium for downstream applications.
138
139 **Traditional bone marrow transplantation (tBMT)**
140 The tBMT was carried out according to our previous description with some modifications[10].
141 Briefly, adult recipient C57BL/6J mice were fed with acid water (PH=2~3) and neomycin (1.1 g/L)
142 for 14 days till receiving 9 Gy X ray treatment. After irradiation, the recipient mice were

143 administrated with GFP-labelled 1 × 10^7 bone marrow cells from the donor through tail vein
144 injection.
145
146 **Microglia replacement by bone marrow transplantation (Mr BMT)**
147 The Mr BMT was carried out according to our previous description with some modifications[20]. In
148 brief, adult recipient C57BL/6J mice were administrated PLX5622 together with acid water
149 (PH=2~3) and neomycin (1.1 g/L) for 2 weeks till receiving 9 Gy X ray treatment. At the same day,
150 the recipient mice were intravenous administrated with GFP-labelled 1 × 10^7 bone marrow cells from
151 the donor through tail vein injection.
152
153 **Statistical analysis**
154 Statistical analyses were conducted using Prism 9 (GraphPad). Each data point represented the
155 average statistical result of three sections in different regions of brain, liver, kidney, lung and spleen.
156 Results were determined independently in double-blind manner. Data were presented as mean ±
157 standard deviation (SD). One-way analysis of variance (ANOVA) with Holm-Sidak's multiple
158 comparisons test (post hoc) was performed for multiple comparisons, while unpaired t test was
159 performed to compare the differences between two groups, unless otherwise stated. Statistical
160 significance was set as $p < 0.05$.
161
162 ***Results***
163 **CSF-1R inhibitor-induced elimination of tissue macrophages**
164 The colony stimulating factor-1 (CSF-1) signalling pathway is known to regulate the development,
165 proliferation, migration, function and survival of myeloid cells, including microglia and peripheral
166 tissue macrophages[21]. The PI3K/Akt pathway has a central role in CSF-1R mediated
167 macrophage survival. In macrophages, Akt can be activated directly through the CSF-1R

168 pTyr721/PI3K pathway and indirectly by ceramide-1-phosphate (C1P) or the Gab2/PI3K
169 pathway, which is counterbalanced by a CSF-1R pTyr559/LynSHIP-1 pathway[22]. Previous
170 study showed that the inhibition of CSF-1R would result in the elimination of microglia in the adult
171 brain and the establishment of a microglia-free niche[23]. Meanwhile, the survival of peripheral
172 tissue-resident macrophages and monocyte are also threatened[18]. Additionally, interference with
173 CSF-1R signalling through depleting *Csf1r* enhancer can lead to the lack of myeloid cells, including
174 the microglia in brain and macrophages in skin, kidney, heart, and peritoneum. However, the other
175 periphery tissue macrophages are unaffected[24].
176
177 The small molecule PLX5622 is a CSF-1R antagonist that has been tested in a range of animal
178 models[23, 25, 26]. Here, adult mice were administered control and PLX5622 chow for 14 days to
179 examine whether CSF-1R inhibition could generate a macrophage-free niche in peripheral tissues
180 within this time window (Fig. 1A). IBA1 was used as a marker to determine the number of microglia
181 in brain and macrophages in peripheral organs, as IBA1 is specifically expressed in most
182 subpopulations of monocyte and macrophage lineage cells[27]. Consistent with previous studies, we
183 observed that PLX5622 treatment resulted in the elimination of ~99% of microglia and the creation
184 of a microglia-free environment in the brain[23]. However, unlike with the observation in brain,
185 44.08% IBA1-positive macrophages were depleted in the liver, 50.58% in the lung, 87.123% in the
186 kidney, 31.41% in the spleen after 14 days PLX5622 treatment (Fig. 1B and Fig. S1). These
187 observations demonstrated that PLX5622 exerted a significant elimination of peripheral tissue
188 macrophages, although its efficiency was lower than in the CNS.
189
190 Although F4/80 is widely used in the analysis of macrophages, it is also expressed in other immune
191 cells, such as dendritic cells (DCs) in the spleen[28]. We evaluated the co-expression rate of F4/80
192 and IBA1 in various tissues. Our results showed that all F4/80^{+} cells expressed IBA1 in the liver, but

193 85.67% F4/80^{+} cells expressed IBA1 in the lung, and 50.17% in the kidney, 92.96% in the spleen
194 (Fig. S2). Additionally, the elimination rate of F4/80-positive cells after PLX5622 treatment varied
195 among tissues, with 44.08% in the liver, 51.62 % in the lung, 97.46% in the kidney, and 36% in the
196 spleen (Fig. 1C and 1D). Interestingly, the absent of F4/80^{+} macrophages in kidney after CSF-1R
197 antagonist treatment was consistent with the findings in *Csf1* enhancer deletion mice[29]. Noticeably,
198 granulocyte-macrophage colony stimulating factor 2 (GM-CSF) , also known as colony stimulating
199 factor-2 (CSF-2) regulates lung macrophage survival together with CSF-1[30]. CSF-2/CSF2RB
200 signalling pathway is also important for alveolar macrophage survival, so inhibiting CSF-1R alone
201 will not kill all alveolar macrophages. As CSF-1/CSF-1R signal pathway is crucial for the
202 proliferation and survival of patrolling monocytes[31, 32], the declined number of IBA1 and F4/80
203 cells in the lung after PLX5622 administration was also likely attributed to the elimination of
204 monocytes.
205
206 **Mr BMT successfully replaced Kupffer cells with BM-derived macrophages in the liver**
207 We previously discovered that microglia-free niche is a prerequisite condition for the successful
208 engraftment of BM-derived cells[10]. We thus hypothesized that the elimination of tissue
209 macrophages by utilization of CSF-1R inhibitor would improve the BM engraftment efficiency. To
210 evaluate the replacement efficiency of macrophages in the liver, we used *Cx3cr1*$^{+/GFP}$ mice as donor,
211 as CX3CR1 is expressed in monocyte/macrophage lineage cells[19]. The recipient mice were fed
212 with PLX5622-formulated chow for 14 days and then subjected to X-ray irradiation, followed by an
213 intravenous injection of 1×10^{7} BMCs from *Cx3cr1*$^{+/GFP}$ as we previously described[11]. After that,
214 the recipient mice were fed with control diet for thirty days to remove the CSF-1R inhibition (Fig.
215 2A). We replaced 98.62% of brain resident microglia with BM-derived microglia-like cells (Fig. S3),
216 indicating that Mr BMT exhibits an exceptionally high level of transplantation effectiveness within

217 the brain. We firstly examined BM-derived macrophages ratio in the peripheral organs of the
218 chimeric mouse, then the morphological changes were also included in the analysis.
219
220 In the adult mouse liver, Kupffer cells (KCs) are originated from yolk sac (YS) and fetal liver
221 monocyte-derived macrophages and replenished independently by monocyte-derived precursors in
222 the steady state[1]. Both cell populations share common macrophage functions, including
223 phagocytosis, pathogen defence, native and adaptive immune regulation. Here, we observed that
224 more than 98.22% of primary KCs were replaced by BM-derived $GFP^{+}IBA1^{+}$ macrophages at thirty
225 days post Mr BMT. There was no significant difference in transplantation efficiency between tBMT
226 and Mr BMT (Fig. 2B-2D). Compared with primary KCs, the body size of the BM-derived KCs was
227 smaller, implying different cell originations of KCs are linked to the discrepancies in cell
228 morphology and function like immune response and tissue repairment ability (Fig. 2E and 2F).
229
230 **Mr BMT strategy showed high replacement efficiency of kidney tissue macrophages**
231 We further tested the macrophage replacement efficiency in the kidney after tBMT and Mr BMT. In
232 the renal, the majority tissue macrophages are derived from YS and fetal liver macrophages, and the
233 YS derived macrophages progressively expand in the mouse kidney with age[33]. These populations
234 are maintained in situ by self-renewal, largely independent of adult haematopoiesis across
235 lifespan[34, 35]. Immunofluorescent (IF) staining of GFP in kidney sections from recipient
236 C57BL/6J mice revealed GFP^{+} BM-derived macrophages spread out the cortex and medulla after
237 tBMT and Mr BMT (Fig. 3A). About 87.22% of tissue macrophages were reconstituted by
238 $GFP^{+}IBA1^{+}$ BM-derived macrophages thirty days after tBMT (Fig. 3B and 3C). After recovery from
239 Mr BMT, more than 87.50% of primary kidney macrophages were successfully colonized by
240 $GFP^{+}IBA1^{+}$ BM-derived macrophages (Fig. 3B-3C), suggesting Mr BMT achieved a similar
241 replacement efficiency to tBMT. Both in tBMT and Mr BMT group, the replacement rate of

242 GFP$^+$F4/80$^+$ / F4/80$^+$ was similar to GFP$^+$IBA1$^+$ / IBA1$^+$ (Fig. 3B-3D). Previous study demonstrated
243 the endogenic macrophages presented a distinct morphology and function compared to BM-derived
244 macrophages[20, 36, 37]. Therefore, we examined the morphology of the newly formed
245 macrophages in the kidney after tBMT and Mr BMT. We observed that the surface area was reduced
246 significantly in BM-derived macrophages, implying BM-macrophages did not fully acquire a
247 resident macrophage phenotype (Fig. 3E and 3F).
248
249 **Mr BMT achieved high engraftment efficiency of macrophages in the lung and spleen**
250 Next, we examined the profile of BM-originated macrophages in the lung either after tBMT or Mr
251 BMT (Fig. 4A). After transplantation, a great number of GFP$^+$ BM-derived cells proliferated in the
252 recipient mouse lung, and subpopulations of them were labelled by macrophage/monocyte lineage
253 marker IBA1 and F4/80. After recovery from tBMT, about 80.70% endogenous
254 macrophages/monocytes cells were replaced by GFP$^+$ F4/80$^+$ BM cells. In Mr BMT group, there
255 were 85.17% IBA1$^+$ and 76.53% F4/80$^+$ cells in the recipient mouse lung were detected as BM-
256 derived GFP$^+$ cells after Mr BMT (Fig. 4B-4D), suggesting comparable replacement efficiency to
257 tBMT. Previous study has demonstrated that CX3CR1$^+$ BMCs could give rise to DCs and supply
258 tissue DCs in lung[38, 39]. We found 2.81% of GFP$^+$ cells that were IBA1$^-$ and F4/80$^-$, which were
259 likely to differentiate into pulmonary DCs (Fig. 4E and 4F). Lung resident macrophage contained
260 alveolar macrophages (AMs) and interstitial macrophages (IMs)[40]. AMs have high expression of
261 CD11c and low expression of CX3CR1[41, 42], which is totally different from the GFP$^+$ cells after
262 tBMT or Mr BMT. Thus, we hypothesized that the replacement cells more likely to convert to IMs
263 after thirty days recovery.
264
265 Lastly, we investigated the replacement efficiency of macrophages/monocytes in the spleen after
266 received *Cx3cr1*$^{+/GFP}$ transplantation (Fig. 5A). Regardless of the approaches used for BMT, the

staining results revealed that more than 50% of tissue-resident macrophages were replaced by GFP^+ BM-derived cells (Fig. 5B-5D). Compared with other peripheral organs, the replacement rate in the spleen was lower, which may be attributed to the different macrophage turnover rate in different organs. However, similar with the observations in other peripheral organs, BM-derived macrophages in the spleen possessed a smaller cell body and less branches, differing from the endogenous embryonic originated macrophages. Additionally, there are 6.96 % GFP^+ cells that were $IBA1^-$ and $F4/80^-$, which were likely to contribute to DCs in the spleen (Fig. 5E and 5F).

Discussion

The Mr BMT approaches a highly efficient strategy for the replenishment of endogenous microglia with BM-derived microglia-like cells at the CNS-wide scale (over 92%) in adult mouse. In contrast, BMCs do not extensively proliferate and engraft the recipient brain (less than 5~20%) by using tBMT method. In current study, we further investigated tissue-resident macrophages replacement efficiency in the peripheral organs by using the Mr BMT approach. Our results demonstrated that BM-derived macrophages efficiently reconstituted tissue macrophages in the liver, kidney, lung and spleen. Although the replacement efficiency had a subtle difference in different organs, which may be attributed to the different turnover rate of tissue-resident macrophages. Thus, Mr BMT achieved a similarly high replacement efficiency comparable to tBMT, but owned higher efficiently in the CNS. These findings suggested that the Mr BMT approach could be a powerful tool for allogenic macrophages replacement in both CNS and peripheral organs. It means that Mr BMT may be a promising cell therapy strategy for a wide range of diseases that affect both central and peripheral myeloid cells, such as ALS and ALD. Despite these encouraging findings, it is important to fully understand the safety of Mr BMT, including its potential long-term effects on tissue macrophage populations and any risks associated with the irradiation used for myelosuppression. Nonetheless,

with continued research and development, the Mr BMT strategy may ultimately offer a powerful tool for the treatment of a range of diseases that affect the immune system.

Ethics approval and consent to participate

All animal experiments were conducted in accordance with the guidelines of the Institutional Animal Care and Use Committee of the Department of Laboratory Animal Science at Fudan University (permit
number: 202110005S).

Declaration of Competing Interest

The authors have no commercial, proprietary or financial interest in the products or companies described in this article.

Author contributions

Y.R. supervised and conceptualized this study. Y.R., and B.Y. wrote the manuscript. B.Y. and Y.H. performed most experiments. B.Y. analysed the staining results, J.D. and Y.H. provided necessary study support. All authors discussed the results and commented on this manuscript. And at last, we appreciate Open AI's assistance in language.

Acknowledgements

The authors thank Yanxia Rao and Bo Peng (Fudan University) for their sponsorship and support of this experiment. Fang Lei and Jiachen Zhu (Fudan University) for the excellent laboratory management. In addition, the authors express their gratitude and respect to all animals sacrificed in this study.

Data Availability Statement:

The raw data supporting the conclusion of this article will be made available by the authors, without undue reservation.

Figures and Tables:

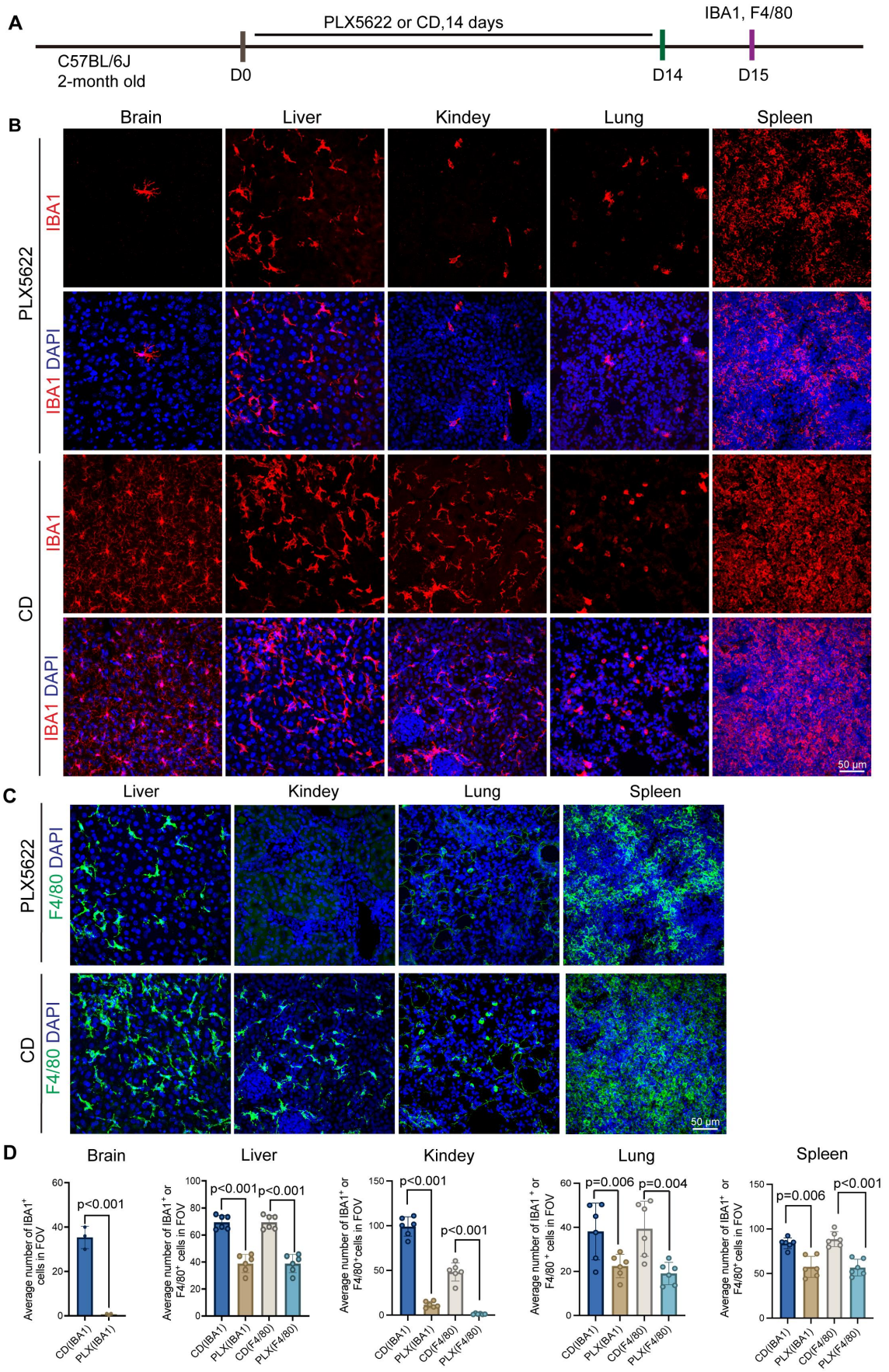

322 **Fig. 1 The CSF-1R antagonist, PLX5622, depleted microglia in the brain and resident**
323 **macrophages in peripheral tissue.** (A) Scheme of time points for microglial depletion and
324 examination time points. (B) Representative images show the depletion efficiency of microglia
325 (IBA1, red) in the brain or peripheral macrophages (IBA1, red) in the peripheral organs following
326 the administration of CD or PLX5622. Scale bar, 50 μm. (C) Representative images show the
327 depletion efficiency of tissue macrophages (F4/80, green) in peripheral organs following the
328 administration of PLX5622. Scale bar, 50 μm. (D) Quantification the average number of $IBA1^+$ cells
329 or $F4/80^+$ cells in the indicated organs. N = 3~6 mice. Two-tailed unpaired test. Data are presented as
330 mean ± SD. CD: control diet; FOV: Field of View; D: day.

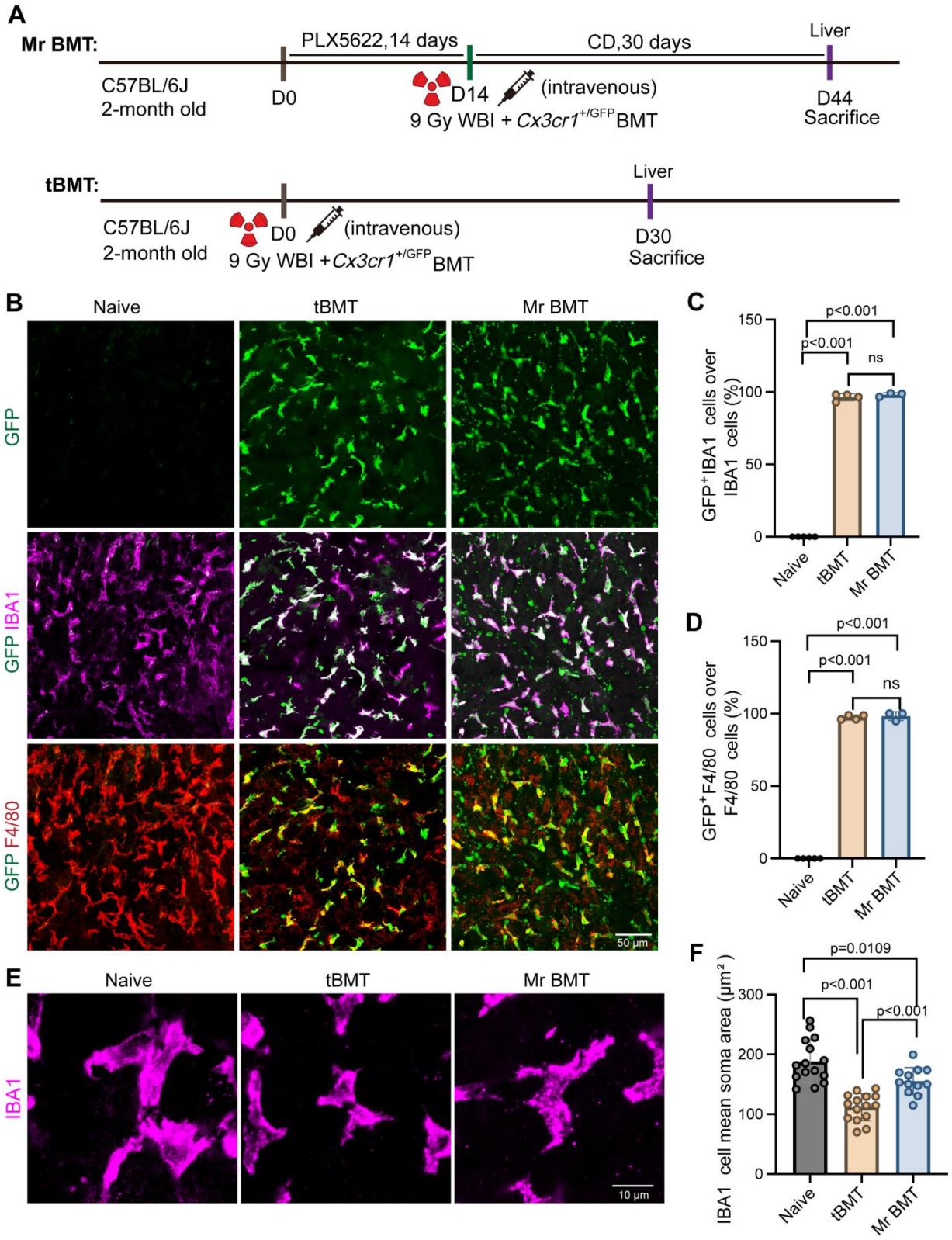

331

332 **Fig. 2 Mr BMT successfully replaced Kupffer cells with BM-derived macrophages in the liver.**

333 (A) Scheme of time points for Mr BMT and tBMT strategy. (B) Representative images show BM-

334 derived cells (GFP, green), liver resident macrophages (IBA1, magenta), liver resident macrophages

335 (F4/80, red) in the liver after tBMT or Mr BMT treatment. Scale bar, 50 μm. (C-D) Quantification
336 the percentage of tBMT-derived cells and Mr BMT-derived cells in the liver. N = 3~5 mice. One-
337 way ANOVA with Holm-Sidak multiple-comparisons test (post hoc). Data are presented as mean ±
338 SD. (E) Representative images show the morphology of BM-derived KCs (IBA1, magenta) in the
339 liver. Scale bar, 10um. (F) Quantification of soma area of $IBA1^{+}$ cells in the liver. N = 3~5 mice. For
340 each mouse, take three non-consecutive sections, and each dot represents one cell. Each dot
341 represents one cell. One-way ANOVA with Holm-Sidak multiple-comparisons test (post hoc). Data
342 are presented as mean ± SD. CD: control diet; WBI: whole brain irradiation; D: day.

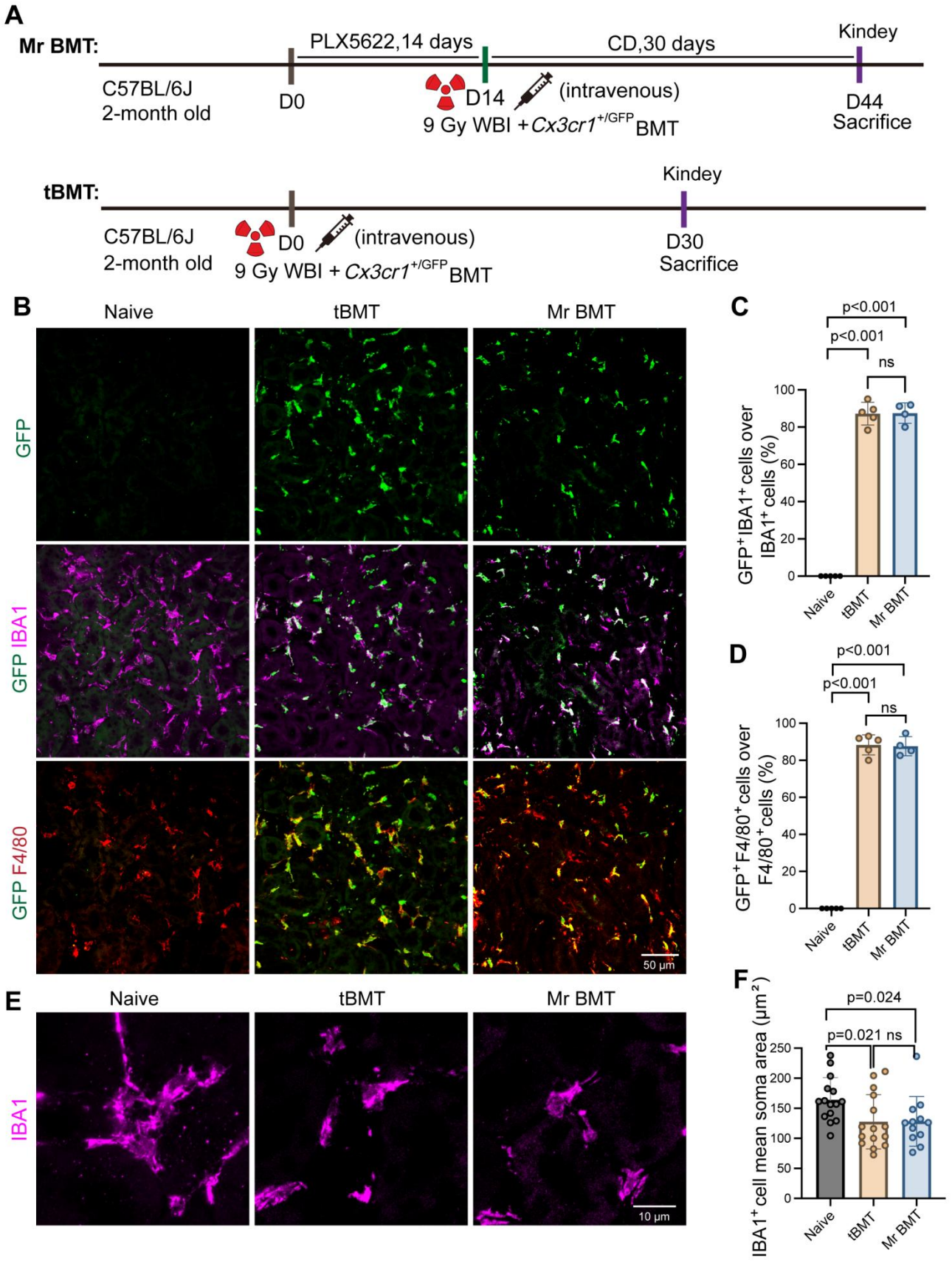
A
Mr BMT:
PLX5622,14 days
CD,30 days
Kindey
C57BL/6J
2-month old
D0
D14
(intravenous)
9 Gy WBI + Cx3cr1+/GFP BMT
D44
Sacrifice
tBMT:
Kindey
C57BL/6J
2-month old
D0
(intravenous)
9 Gy WBI + Cx3cr1+/GFP BMT
D30
Sacrifice
B
Naive
tBMT
Mr BMT
GFP
GFP IBA1
GFP F4/80
50 μm
C
p<0.001
p<0.001
ns
GFP+IBA1+ cells over IBA1+ cells (%)
Naive
tBMT
Mr BMT
D
p<0.001
p<0.001
ns
GFP+F4/80+cells over F4/80+cells (%)
Naive
tBMT
Mr BMT
E
Naive
tBMT
Mr BMT
IBA1
10 μm
F
p=0.024
p=0.021 ns
IBA1+cell mean soma area (μm2)
Naive
tBMT
Mr BMT

343

344 **Fig. 3 Evaluate the efficiency of the Mr BMT strategy in replacing macrophages in kidney.** (A)
345 Scheme of time points for Mr BMT and tBMT strategy. (B) Representative images show BM-
346 derived cells (GFP, green), kidney resident macrophages (IBA1, magenta), kidney resident
347 macrophages (F4/80, red) in the kideney after tBMT or Mr BMT treatment. Scale bar, 50 μm. (C-D)
348 Quantification the percentage of tBMT-derived cells or Mr BMT-derived cells in the kidney. N =
349 4~5 mice. One-way ANOVA with Holm-Sidak multiple-comparisons test (post hoc). Data are
350 presented as mean ± SD. (E) Representative images showing the morphology of BM-derived kidney
351 macrophages (IBA1, magenta) in the kidney. Scale bar, 10 μm. (F) Quantification of soma area of
352 $IBA1^{+}$ cells in the kidney. N = 4~5 mice. For each mouse, take three non-consecutive sections, and
353 each dot represents one cell. Each dot represents one cell. One-way ANOVA with Holm-Sidak
354 multiple-comparisons test (post hoc). Data are presented as mean ± SD. CD: control diet; WBI:
355 whole brain irradiation; D: day.

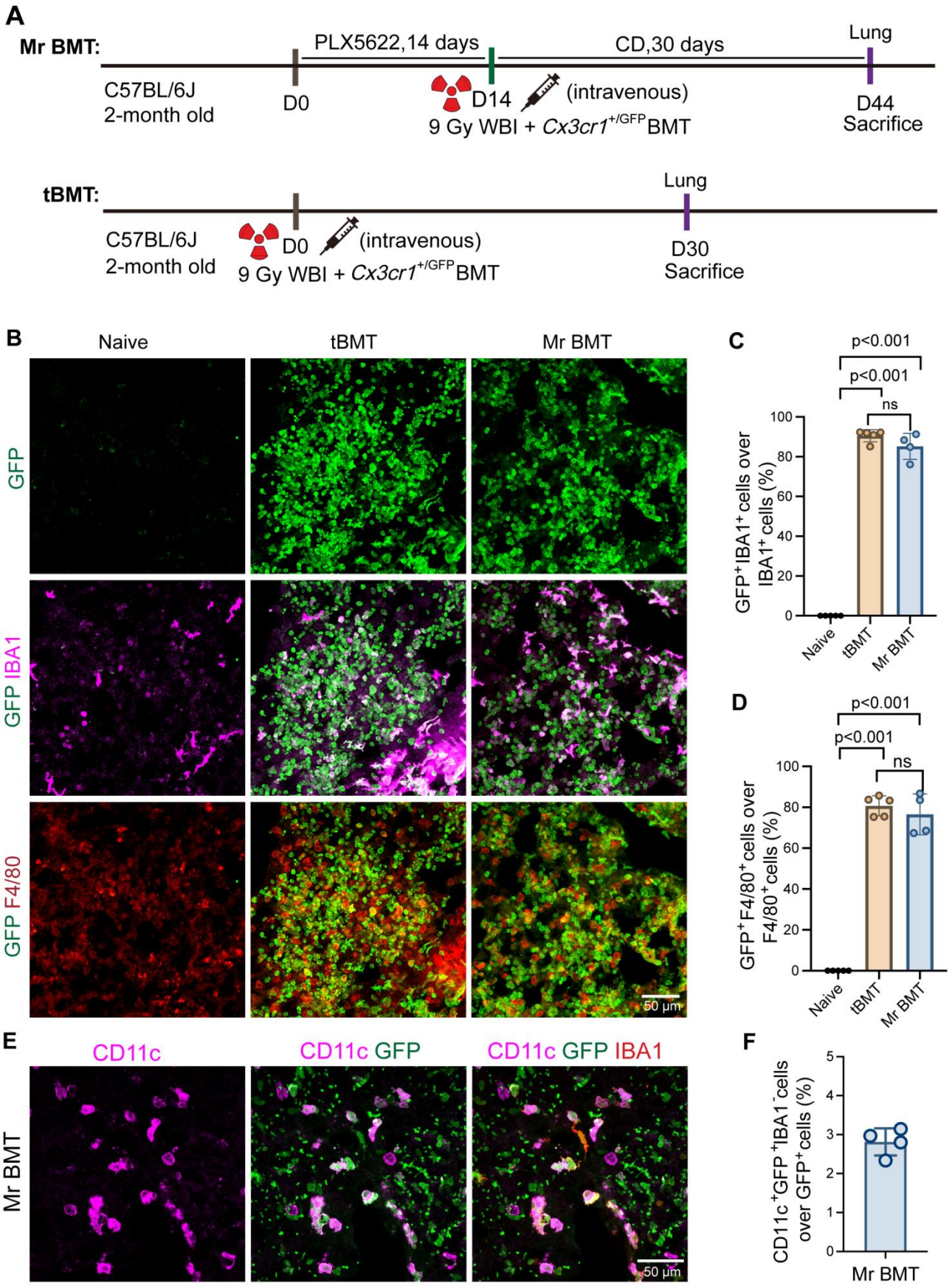
A
Mr BMT:
PLX5622,14 days
CD,30 days
Lung
C57BL/6J
2-month old
D0
D14
(intravenous)
9 Gy WBI + Cx3cr1+/GFP BMT
D44
Sacrifice
tBMT:
Lung
C57BL/6J
2-month old
D0
(intravenous)
9 Gy WBI + Cx3cr1+/GFP BMT
D30
Sacrifice
B
Naive
tBMT
Mr BMT
GFP
GFP IBA1
GFP F4/80
50 μm
C
p<0.001
p<0.001
ns
GFP+IBA1+ cells over IBA1+ cells (%)
Naive
tBMT
Mr BMT
D
p<0.001
p<0.001
ns
GFP+F4/80+ cells over F4/80+ cells (%)
Naive
tBMT
Mr BMT
E
CD11c
CD11c GFP
CD11c GFP IBA1
Mr BMT
50 μm
F
CD11c+GFP+IBA1- cells over GFP+ cells (%)
Mr BMT

356

357 **Fig. 4 Evaluate the replacement efficiency of lung tissue-resident macrophages under Mr BMT**
358 **treatmet.** (A) Scheme of time points for Mr BMT and tBMT strategy. (B) Representative images
359 show BM-derived cells (GFP, green), lung resident macrophages (IBA1, magenta), lung resident
360 macrophages (F4/80, red) in the lung after tBMT or Mr BMT treatment. Scale bar, 50 μm. (C-D)
361 Quantification the percentage of tBMT-derived cells or Mr BMT-derived cells in the lung. N = 4~5
362 mice. One-way ANOVA with Holm-Sidak multiple-comparisons test (post hoc). Data are presented
363 as mean ± SD. (E) Representative images show myeloid cells (CD11c, magenta), BM-derived cells
364 (GFP, green) and lung tissue-resident macrophages (IBA1, red) in the lung after Mr BMT. Scale bar,
365 50 μm. (F) Quantification the ratio of $CD11c^{+}$ GFP^{+} $IBA1^{-}$ cells / GFP^{+} cells in the lung after Mr
366 BMT. N = 4 mice. Data are presented as mean ± SD. CD: control diet; WBI: whole brain irradiation;
367 D: day.

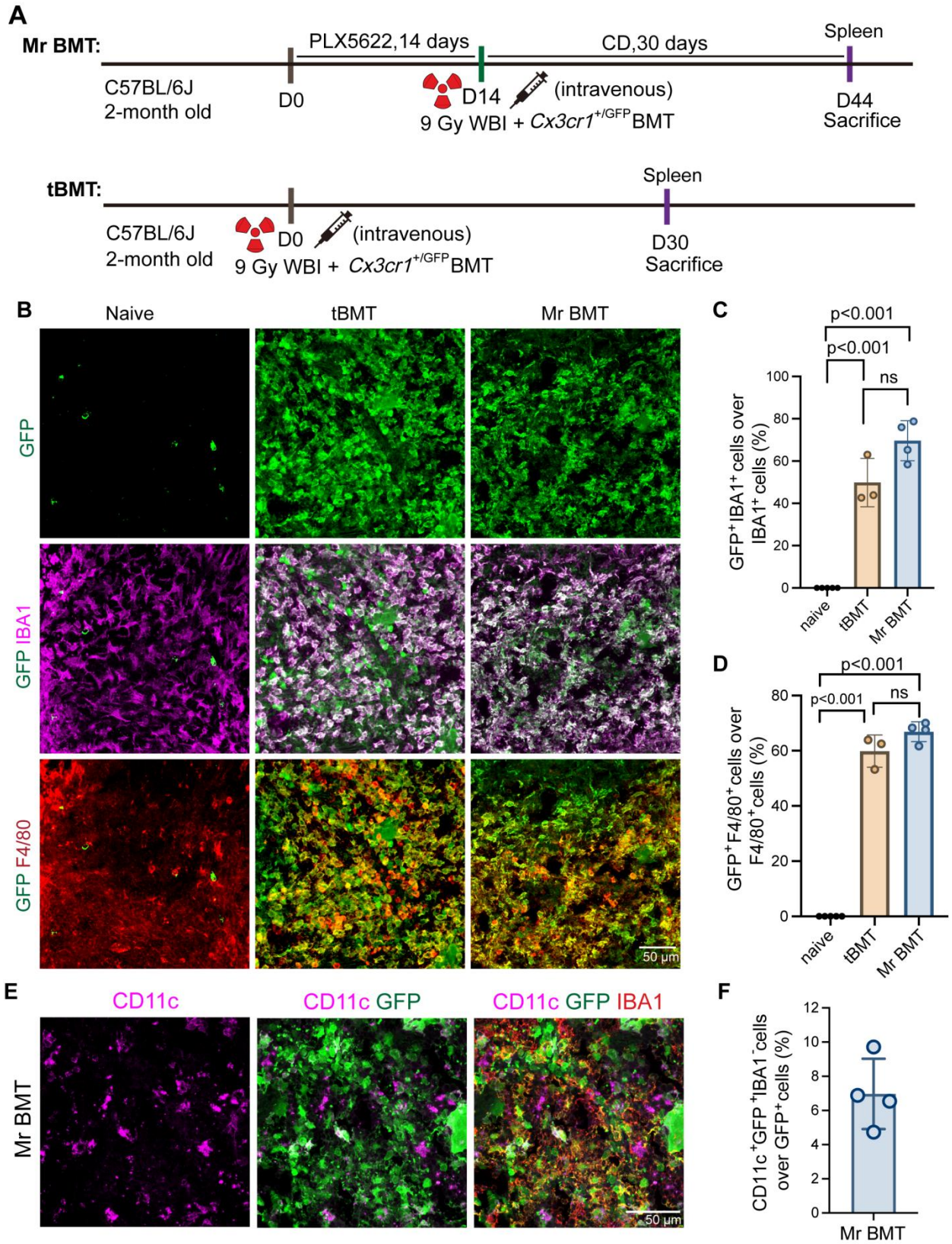

Fig. 5 Replacement efficiency of spleen tissue-resident macrophages under Mr BMT treatmet. (A) Scheme of time points for Mr BMT and tBMT strategy. (B) Representative images show BM-

371 derived cells (GFP, green), spleen resident macrophages (IBA1, magenta), spleen resident
372 macrophages (F4/80, red) in the liver after tBMT or Mr BMT treatment. Scale bar, 50 μm. (C-D)
373 Quantification the percentage of tBMT-derived cell or Mr BMT cell percentage in the spleen. N =
374 3~5 mice. One-way ANOVA with Holm-Sidak multiple-comparisons test (post hoc). Data are
375 presented as mean ± SD. (E) Representative images show myeloid cells (CD11c, magenta), BM-
376 derived cells (GFP, green) and spleen tissue-resident macrophages (IBA1, red) in the spleen after Mr
377 BMT. Scale bar, 50 μm. (F) Quantification the ratio of $CD11c^{+}$ GFP^{+} $IBA1^{-}$ cells / GFP^{+} cells in the
378 spleen after Mr BMT. N = 4 mice. Data are presented as mean ± SD. CD: control diet; WBI: whole
379 brain irradiation; D: day.

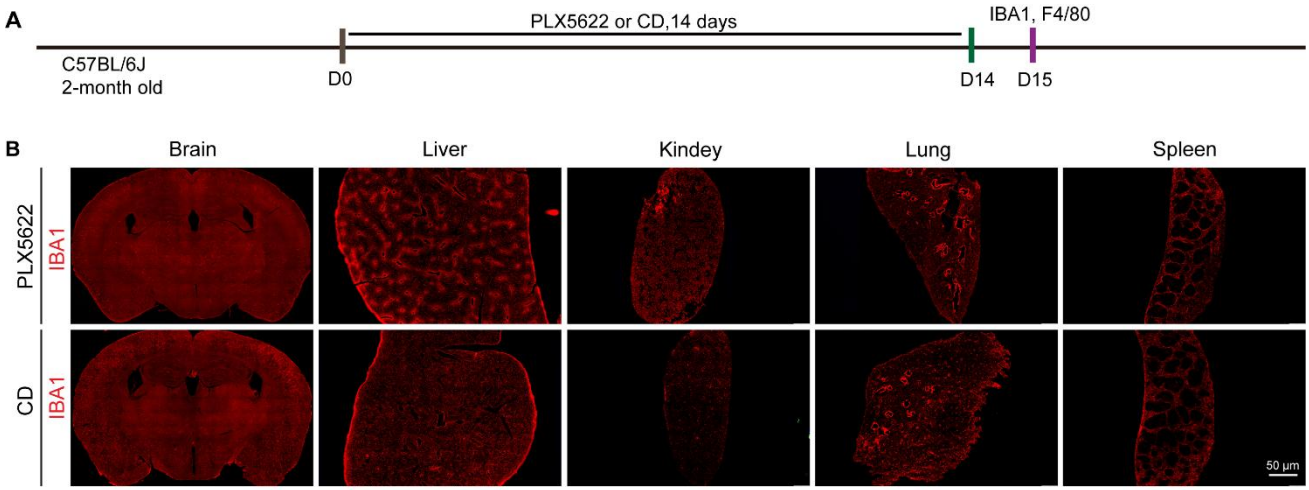

380

381 **Fig. S1 PLX5622 depleted microglia in CNS and resident macrophages in peripheral organs.**
382 (A) Scheme of time points for microglial depletion and examination time points. (B) Representative
383 images show the depletion efficiency of microglia (IBA1, red) in the whole brain or macrophages
384 (IBA1, red) in the peripheral organs following the administration of CD or PLX5622. Scale bar, 50
385 μm. CD: control diet; D: day.

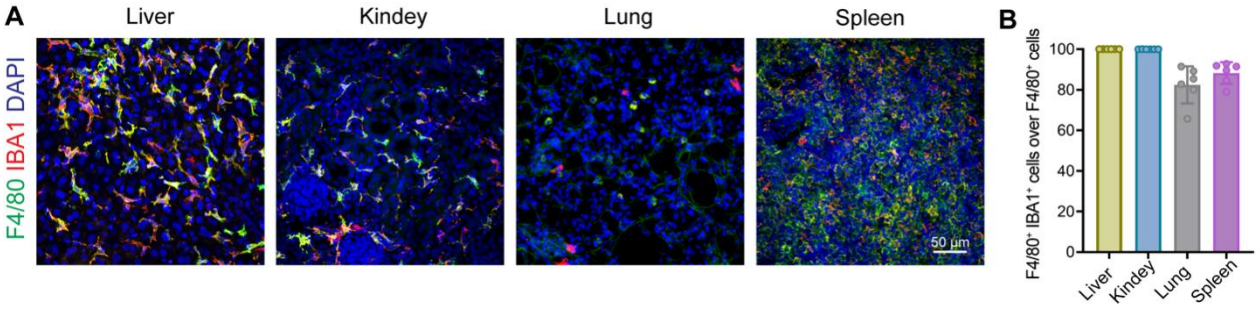

Fig. S2 The co-lable rate of F4/80 and IBA1 in peripheral tissues. (A) Representative images show the co-labeling of F4/80 and IBA1 in the peripheral organs of naïve group. (B) Quantification the percentage of F4/80^{+} IBA1^{+} cells over IBA1^{+} cells in different peripheral tissues. N = 6 mice. Data are presented as mean ± SD. Scale bar, 50 μm.

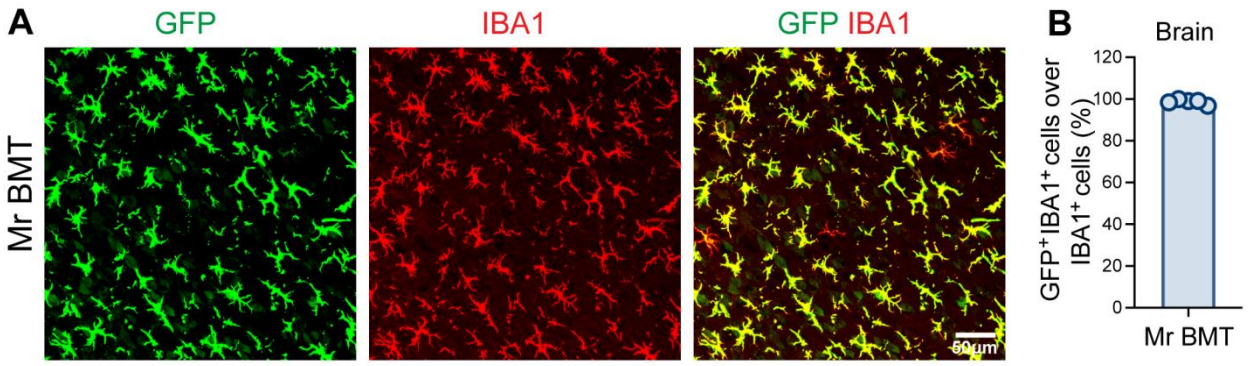

Fig. S3 The replacement efficiency of Mr BMT in the brain was higher than in peripheral. (A) Representative images show the engrafted BM-derived microglia-like cells (GFP, green) in the brain after Mr BMT. Scale bar, 50 μm. (B) Quantification the percentage of Mr BMT-derived cells in the brain. N =5 mice. Data are presented as mean ± SD.

410

411 ***References***

412 1. Epelman S, Lavine KJ, Randolph GJ. Origin and functions of tissue macrophages. *Immunity*
413 2014; **41**(1)**:** 21-35. e-pub ahead of print 2014/07/19; doi: 10.1016/j.immuni.2014.06.013

414 2. Ginhoux F, Guilliams M. Tissue-Resident Macrophage Ontogeny and Homeostasis. *Immunity*
415 2016; **44**(3)**:** 439-449. e-pub ahead of print 2016/03/18; doi: 10.1016/j.immuni.2016.02.024

416 3. Hashimoto D, Chow A, Noizat C, Teo P, Beasley MB, Leboeuf M *et al.* Tissue-resident
417 macrophages self-maintain locally throughout adult life with minimal contribution from
418 circulating monocytes. *Immunity* 2013; **38**(4)**:** 792-804. e-pub ahead of print 2013/04/23; doi:
419 10.1016/j.immuni.2013.04.004

420 4. Wynn TA, Chawla A, Pollard JW. Macrophage biology in development, homeostasis and
421 disease. *Nature* 2013; **496**(7446)**:** 445-455. e-pub ahead of print 2013/04/27; doi:
422 10.1038/nature12034

423 5. Fischer A. Thirty years of bone marrow transplantation for severe combined
424 immunodeficiency. *The New England journal of medicine* 1999; **340**(7)**:** 559-561. e-pub
425 ahead of print 1999/02/18; doi: 10.1056/nejm199902183400711

426 6. Levite M, Zinger H, Zisman E, Reisner Y, Mozes E. Beneficial effects of bone marrow
427 transplantation on the serological manifestations and kidney pathology of experimental
428 systemic lupus erythematosus. *Cellular immunology* 1995; **162**(1)**:** 138-145. e-pub ahead of
429 print 1995/04/15; doi: 10.1006/cimm.1995.1061

430 7. Kushida T, Ueda Y, Umeda M, Oe K, Okamoto N, Iida H *et al.* Allogeneic intra-bone marrow
431 transplantation prevents rheumatoid arthritis in SKG/Jcl mice. *Journal of autoimmunity* 2009;
432 **32**(3-4)**:** 216-222. e-pub ahead of print 2009/04/08; doi: 10.1016/j.jaut.2009.02.015

433 8. Zhang S, Dai Q, Zhang B, Liu S, Wang Y, Zhang Y *et al.* Syngeneic bone marrow
434 transplantation in combination with PI3K inhibitor reversed hyperglycemia in later-stage

435 streptozotocin-induced diabetes. *Annals of translational medicine* 2021; **9**(22)**:** 1642. e-pub
436 ahead of print 2022/01/07; doi: 10.21037/atm-21-3329
437 9. Boffa G, Signori A, Massacesi L, Mariottini A, Sbragia E, Cottone S *et al.* Hematopoietic
438 Stem Cell Transplantation in People With Active Secondary Progressive Multiple Sclerosis.
439 *Neurology* 2023; **100**(11)**:** e1109-e1122. e-pub ahead of print 2022/12/22; doi:
440 10.1212/wnl.0000000000206750
441 10. Xu Z, Rao Y, Huang Y, Zhou T, Feng R, Xiong S *et al.* Efficient Strategies for Microglia
442 Replacement in the Central Nervous System. *Cell reports* 2020; **33**(8)**:** 108443. e-pub ahead
443 of print 2020/11/26; doi: 10.1016/j.celrep.2020.108443
444 11. Xu Z, Zhou X, Peng B, Rao Y. Microglia replacement by bone marrow transplantation (Mr
445 BMT) in the central nervous system of adult mice. *STAR protocols* 2021; **2**(3)**:** 100666. e-pub
446 ahead of print 2021/07/22; doi: 10.1016/j.xpro.2021.100666
447 12. Xu Z, Rao Y, Peng B. Protocol for microglia replacement by peripheral blood (Mr PB). *STAR*
448 *protocols* 2021; **2**(2)**:** 100613. e-pub ahead of print 2021/06/29; doi:
449 10.1016/j.xpro.2021.100613
450 13. Yoo Y, Neumayer G, Shibuya Y, Mader MM, Wernig M. A cell therapy approach to restore
451 microglial Trem2 function in a mouse model of Alzheimer's disease. *Cell stem cell* 2023;
452 **30**(8)**:** 1043-1053.e1046. e-pub ahead of print 2023/08/05; doi: 10.1016/j.stem.2023.07.006
453 14. Shibuya Y, Kumar KK, Mader MM, Yoo Y, Ayala LA, Zhou M *et al.* Treatment of a genetic
454 brain disease by CNS-wide microglia replacement. *Science translational medicine* 2022;
455 **14**(636)**:** eabl9945. e-pub ahead of print 2022/03/17; doi: 10.1126/scitranslmed.abl9945
456 15. Colella P, Sayana R, Suarez-Nieto MV, Sarno J, Nyame K, Xiong J *et al.* CNS Repopulation
457 by Hematopoietic-Derived Microglia-Like Cells Corrects Progranulin deficiency. *Research*
458 *square* 2023. e-pub ahead of print 2023/10/04; doi: 10.21203/rs.3.rs-3263412/v1
459 16. Manickam V, Gawande DY, Stothert AR, Clayman AC, Batalkina L, Warchol ME *et al.*

460 Macrophages Promote Repair of Inner Hair Cell Ribbon Synapses following Noise-Induced
461 Cochlear Synaptopathy. *The Journal of neuroscience : the official journal of the Society for*
462 *Neuroscience* 2023; **43**(12)**:** 2075-2089. e-pub ahead of print 2023/02/23; doi:
463 10.1523/jneurosci.1273-22.2023
464 17. Li Y, Ritzel RM, Khan N, Cao T, He J, Lei Z *et al.* Delayed microglial depletion after spinal
465 cord injury reduces chronic inflammation and neurodegeneration in the brain and improves
466 neurological recovery in male mice. *Theranostics* 2020; **10**(25)**:** 11376-11403. e-pub ahead of
467 print 2020/10/15; doi: 10.7150/thno.49199
468 18. Spiteri AG, Ni D, Ling ZL, Macia L, Campbell IL, Hofer MJ *et al.* PLX5622 Reduces
469 Disease Severity in Lethal CNS Infection by Off-Target Inhibition of Peripheral
470 Inflammatory Monocyte Production. *Frontiers in immunology* 2022; **13:** 851556. e-pub
471 ahead of print 2022/04/12; doi: 10.3389/fimmu.2022.851556
472 19. Jung S, Aliberti J, Graemmel P, Sunshine MJ, Kreutzberg GW, Sher A *et al.* Analysis of
473 fractalkine receptor CX(3)CR1 function by targeted deletion and green fluorescent protein
474 reporter gene insertion. *Mol Cell Biol* 2000; **20**(11)**:** 4106-4114. e-pub ahead of print
475 2000/05/11; doi: 10.1128/mcb.20.11.4106-4114.2000
476 20. Brochu S, Perreault C, Bélanger R. Evaluation of Fc-dependent monocyte-macrophage
477 function in bone marrow transplant recipients. *Experimental hematology* 1989; **17**(9)**:** 948-
478 951. e-pub ahead of print 1989/10/01;
479 21. Hume DA, MacDonald KP. Therapeutic applications of macrophage colony-stimulating
480 factor-1 (CSF-1) and antagonists of CSF-1 receptor (CSF-1R) signaling. *Blood* 2012; **119**(8)**:**
481 1810-1820. e-pub ahead of print 2011/12/22; doi: 10.1182/blood-2011-09-379214
482 22. Stanley ER, Chitu V. CSF-1 receptor signaling in myeloid cells. *Cold Spring Harbor*
483 *perspectives in biology* 2014; **6**(6). e-pub ahead of print 2014/06/04; doi:
484 10.1101/cshperspect.a021857

485 23. Huang Y, Xu Z, Xiong S, Sun F, Qin G, Hu G *et al.* Repopulated microglia are solely derived
486 from the proliferation of residual microglia after acute depletion. *Nature neuroscience* 2018;
487 **21**(4)**:** 530-540. e-pub ahead of print 2018/02/24; doi: 10.1038/s41593-018-0090-8
488 24. Rojo R, Raper A, Ozdemir DD, Lefevre L, Grabert K, Wollscheid-Lengeling E *et al.* Deletion
489 of a Csf1r enhancer selectively impacts CSF1R expression and development of tissue
490 macrophage populations. *Nature communications* 2019; **10**(1)**:** 3215. e-pub ahead of print
491 2019/07/22; doi: 10.1038/s41467-019-11053-8
492 25. Arreola MA, Soni N, Crapser JD, Hohsfield LA, Elmore MRP, Matheos DP *et al.* Microglial
493 dyshomeostasis drives perineuronal net and synaptic loss in a CSF1R(+/-) mouse model of
494 ALSP, which can be rescued via CSF1R inhibitors. *Science advances* 2021; **7**(35). e-pub
495 ahead of print 2021/08/27; doi: 10.1126/sciadv.abg1601
496 26. Spangenberg E, Severson PL, Hohsfield LA, Crapser J, Zhang J, Burton EA *et al.* Sustained
497 microglial depletion with CSF1R inhibitor impairs parenchymal plaque development in an
498 Alzheimer's disease model. *Nature communications* 2019; **10**(1)**:** 3758. e-pub ahead of print
499 2019/08/23; doi: 10.1038/s41467-019-11674-z
500 27. Wächter C, Eiden LE, Naumann N, Depboylu C, Weihe E. Loss of cerebellar neurons in the
501 progression of lentiviral disease: effects of CNS-permeant antiretroviral therapy. *Journal of*
502 *neuroinflammation* 2016; **13**(1)**:** 272. e-pub ahead of print 2016/10/16; doi: 10.1186/s12974-
503 016-0726-0
504 28. Leenen PJ, Radosević K, Voerman JS, Salomon B, van Rooijen N, Klatzmann D *et al.*
505 Heterogeneity of mouse spleen dendritic cells: in vivo phagocytic activity, expression of
506 macrophage markers, and subpopulation turnover. *Journal of immunology (Baltimore, Md. :*
507 *1950)* 1998; **160**(5)**:** 2166-2173. e-pub ahead of print 1998/03/14;
508 29. Lenda DM, Kikawada E, Stanley ER, Kelley VR. Reduced macrophage recruitment,
509 proliferation, and activation in colony-stimulating factor-1-deficient mice results in decreased

510 tubular apoptosis during renal inflammation. *Journal of immunology (Baltimore, Md. : 1950)*
511 2003; **170**(6)**:** 3254-3262. e-pub ahead of print 2003/03/11; doi:
512 10.4049/jimmunol.170.6.3254
513 30. McCowan J, Fercoq F, Kirkwood PM, T'Jonck W, Hegarty LM, Mawer CM *et al.* The
514 transcription factor EGR2 is indispensable for tissue-specific imprinting of alveolar
515 macrophages in health and tissue repair. *Science immunology* 2021; **6**(65)**:** eabj2132. e-pub
516 ahead of print 2021/11/20; doi: 10.1126/sciimmunol.abj2132
517 31. Bonfield TL, Thomassen MJ, Farver CF, Abraham S, Koloze MT, Zhang X *et al.* Peroxisome
518 proliferator-activated receptor-gamma regulates the expression of alveolar macrophage
519 macrophage colony-stimulating factor. *Journal of immunology (Baltimore, Md. : 1950)* 2008;
520 **181**(1)**:** 235-242. e-pub ahead of print 2008/06/21; doi: 10.4049/jimmunol.181.1.235
521 32. Rietkötter E, Bleckmann A, Bayerlová M, Menck K, Chuang HN, Wenske B *et al.* Anti-CSF-
522 1 treatment is effective to prevent carcinoma invasion induced by monocyte-derived cells but
523 scarcely by microglia. *Oncotarget* 2015; **6**(17)**:** 15482-15493. e-pub ahead of print
524 2015/06/23; doi: 10.18632/oncotarget.3855
525 33. Ide S, Yahara Y, Kobayashi Y, Strausser SA, Ide K, Watwe A *et al.* Yolk-sac-derived
526 macrophages progressively expand in the mouse kidney with age. *eLife* 2020; **9**. e-pub ahead
527 of print 2020/04/18; doi: 10.7554/eLife.51756
528 34. Mass E, Ballesteros I, Farlik M, Halbritter F, Günther P, Crozet L *et al.* Specification of
529 tissue-resident macrophages during organogenesis. *Science (New York, N.Y.)* 2016; **353**(6304).
530 e-pub ahead of print 2016/08/06; doi: 10.1126/science.aaf4238
531 35. Ginhoux F, Greter M, Leboeuf M, Nandi S, See P, Gokhan S *et al.* Fate mapping analysis
532 reveals that adult microglia derive from primitive macrophages. *Science (New York, N.Y.)*
533 2010; **330**(6005)**:** 841-845. e-pub ahead of print 2010/10/23; doi: 10.1126/science.1194637
534 36. Hubbard LL, Wilke CA, White ES, Moore BB. PTEN limits alveolar macrophage function

535 against Pseudomonas aeruginosa after bone marrow transplantation. *American journal of*
536 *respiratory cell and molecular biology* 2011; **45**(5)**:** 1050-1058. e-pub ahead of print
537 2011/04/30; doi: 10.1165/rcmb.2011-0079OC
538 37. Chiot A, Zaïdi S, Iltis C, Ribon M, Berriat F, Schiaffino L *et al.* Modifying macrophages at
539 the periphery has the capacity to change microglial reactivity and to extend ALS survival.
540 *Nature neuroscience* 2020; **23**(11)**:** 1339-1351. e-pub ahead of print 2020/10/21; doi:
541 10.1038/s41593-020-00718-z
542 38. Jakubzick C, Tacke F, Ginhoux F, Wagers AJ, van Rooijen N, Mack M *et al.* Blood monocyte
543 subsets differentially give rise to CD103+ and CD103- pulmonary dendritic cell populations.
544 *Journal of immunology (Baltimore, Md. : 1950)* 2008; **180**(5)**:** 3019-3027. e-pub ahead of
545 print 2008/02/23; doi: 10.4049/jimmunol.180.5.3019
546 39. del Rio ML, Rodriguez-Barbosa JI, Bölter J, Ballmaier M, Dittrich-Breiholz O, Kracht M *et*
547 *al.* CX3CR1+ c-kit+ bone marrow cells give rise to CD103+ and CD103- dendritic cells with
548 distinct functional properties. *Journal of immunology (Baltimore, Md. : 1950)* 2008; **181**(9)**:**
549 6178-6188. e-pub ahead of print 2008/10/23; doi: 10.4049/jimmunol.181.9.6178
550 40. Aegerter H, Lambrecht BN, Jakubzick CV. Biology of lung macrophages in health and
551 disease. *Immunity* 2022; **55**(9)**:** 1564-1580. e-pub ahead of print 2022/09/15; doi:
552 10.1016/j.immuni.2022.08.010
553 41. Yu YR, Hotten DF, Malakhau Y, Volker E, Ghio AJ, Noble PW *et al.* Flow Cytometric
554 Analysis of Myeloid Cells in Human Blood, Bronchoalveolar Lavage, and Lung Tissues. *Am*
555 *J Respir Cell Mol Biol* 2016; **54**(1)**:** 13-24. e-pub ahead of print 2015/08/13; doi:
556 10.1165/rcmb.2015-0146OC
557 42. Todd EM, Zhou JY, Szasz TP, Deady LE, D'Angelo JA, Cheung MD *et al.* Alveolar
558 macrophage development in mice requires L-plastin for cellular localization in alveoli. *Blood*
559 2016; **128**(24)**:** 2785-2796. e-pub ahead of print 2016/10/21; doi: 10.1182/blood-2016-03-

705962